Scattering of thermal He beams by crossed atomic and molecular beams. IV. Spherically symmetric intermolecular potentials for $He+CH_4$, NH_3, H_2O, SF_6[a)]

John T. Slankas,[b)] Mark Keil, and Aron Kuppermann

Arthur Amos Noyes Laboratory of Chemical Physics,[c)] California Institute of Technology, Pasadena, California 91125
(Received 6 June 1978)

Differential scattering cross sections are measured for $He+CH_4$, NH_3, H_2O, and SF_6, using the crossed molecular beams technique. These data, which are sensitive to the van der Waals attractive minima and adjacent regions of the intermolecular potential, are interpreted in terms of central-field models. No evidence is found for quenching of the observed diffraction oscillations. The interactions of the isoelectronic hydrides CH_4, NH_3, H_2O with He are found to have decreasing van der Waals radii in this sequence, and their attractive wells all have similar depths. However, the $He+SF_6$ attractive well is found to be anomalously deep, and provides a counter example to the supposition that only the polarizability of the least polarizable of the interacting partners (atoms or molecules) correlates with the van der Waals well depth. Simple combination rules for predicting unlike-pair potential parameters from the corresponding like-pair ones are tested and found inadequate.

I. INTRODUCTION

In recent years, a considerable amount of work has been done, both experimentally[1] and theoretically,[2] to improve our knowledge of interatomic potentials for van der Waals interactions.[3] Molecular beam elastic scattering experiments yield information about these weakly attractive potentials at a level of detail inaccessible to many other techniques, especially for highly quantum systems.[3c,4,5] Potentials for such systems are now well characterized, enabling experimental data of many different kinds to be correlated and accurately described.[4,6,7] However, relatively little is known about atom–molecule or molecule–molecule van der Waals potentials, especially with regard to their orientation dependence.[8–11]

In the present paper we analyze experimental measurements of the differential cross sections (DCS) for the highly quantum systems $He+CH_4$, NH_3, H_2O, and SF_6, using room-temperature crossed beams. The first three molecules represent an isoelectronic series, progressing from nonpolar CH_4 to the highly polar NH_3 and H_2O. The $He+SF_6$ system is an example of the interaction between an atom and a highly symmetric large molecule. In this sense, the $He+CH_4$, NH_3, and H_2O interactions span an interesting transition from a highly symmetric molecule to ones having rather asymmetric nuclear arrangements.

In Sec. II we briefly describe the apparatus used to measure DCS's, and the data reduction procedures used to analyze them. The DCS measurements, and the intermolecular potentials extracted from them, are presented in Sec. III. The importance of anisotropic contributions (or lack thereof) to the measured potentials is discussed in Sec. IV, where we also compare our results with those of different experiments. Systematic trends in the potentials for the systems of this study are discussed. Finally, we summarize our findings in Sec. V.

II. EXPERIMENTAL AND DATA REDUCTION

The crossed molecular beam apparatus used in this investigation has been described previously,[4,8c,12] and only its major components are discussed here. The modulated He primary beam comes from a room-temperature nozzle source, and is angularly well collimated in two stages of differential pumping. Secondary beams of the various gases studied emerge from a glass capillary array, directly into the scattering chamber, and are intense but only slightly supersonic. This beam source may be tilted upwards, thus uncrossing the beams and allowing measurements of the modulated primary beam scattered by background gas. Beam operating characteristics are summarized in Table I. We note that the secondary beam velocity distributions are best described by a Mach number of 1.5 and an "effective" specific heat ratio of 1.64,[13] indicating only very slight cooling of internal states; thus the rotational temperature is presumably close to the ambient one (298 K).

A doubly-differentially pumped quadrupole mass spectrometer, scanning out-of-plane angles (with the in-plane scattering angle set to zero), is used to detect scattered He atoms. Angular spacings between the observed diffraction oscillations are slightly greater for this selection of scattering geometry than for the in-plane scanning geometry that the apparatus also permits. The out-of-plane geometry also allows a more straightforward verification of the symmetry for scattering on both sides of the primary beam, since coordinate frame transformations are not required for this purpose. This symmetry is exploited, as in previous work, to yield scattering angle measurements accurate to within ~0.03°.[4] A 14-stage Cu–Be dynode multiplier is used for ion detection in the analogue mode. Its output is processed by several stages of preamplification, followed by phase-sensi-

[a)] This work was supported in part by a Contract (EY-76-S-03-767) from the Department of Energy. Report Code: CALT-767P4-175.
[b)] Work performed in partial fulfillment of the requirements for the Ph.D. degree in Chemistry at the California Institute of Technology.
[c)] Contribution No. 5798.

 0021-9606/79/031482-10$01.00

TABLE I. Beam operating conditions.

Characteristic	Primary beam	Secondary beams			
Beam gas	He	CH_4	NH_3	H_2O	SF_6
Inlet pressure/torr	1300	2.9	4.8	4.1	3.9
Inlet temperature/K	298	298	298	298	298
Angular FWHM[a]/deg	1	4	6	6	3
Most probable velocity/(km/s)	1.757	0.792	0.769	0.747	0.262
Velocity FWHM,[a] $\Delta v/v$	0.10	0.75	0.75	0.75	0.75
Mach number[13]	18	1.5	1.5	1.5	1.5

[a]Full width at half maximum.

tive lock-in amplification, with the reference of the lock-in synchronized with the primary beam chopper. The output of the lock-in amplifier is digitized for sampling and averaging by a laboratory minicomputer, which also performs background signal subtraction by uncrossing the beams and remeasuring the modulated signal. With liquid-helium cryopumping in the ionizer region of the mass spectrometer, background pressures of $\lesssim 5 \times 10^{-10}$ torr were realized for these experiments. For the $He + CH_4$, NH_3, and H_2O experiments, total integration times at each scattering angle, representing data accumulated over several days' experimentation, ranged from ~2 min near 3°, to ~20 min at the widest angles. Corresponding signal-to-noise ratios were about 40 and 6, respectively. Because of its larger scattering cross section, the same signal-to-noise ratios could be attained for the $He + SF_6$ experiment with only $\sim\frac{2}{3}$ of the total integration times used for the hydride scattering partners.

Maintaining the scattering chamber pressure below $\sim 3\times10^{-6}$ torr, and keeping the primary beam attenuation due to scattering by the secondary beam at $\lesssim 5\%$, ensures that the single-collision conditions essential for DCS measurements prevail. Rapid cryopumping of NH_3 and H_2O on liquid-nitrogen cooled surfaces in the scattering chamber allowed the use of somewhat higher secondary beam pressures for these gases, which however, increased these beams' angular divergences somewhat (see Table I). Periodic mass spectrometric checks of the secondary beams revealed their high purity for all the scattering experiments. In particular, a careful check was made for dimers of the particularly condensable NH_3 and H_2O beams. No dimerization was detected down to the estimated sensitivity limit of $\sim 10^{-7}$ relative to the monomer, despite the integrity of (for example) H_2O ionic polymers as produced by electron-impact ionization.[14]

Scattered primary beam signals were measured between ~2.8° and ~18° (for CH_4, NH_3, and H_2O) or 15.3° (for SF_6) above the plane of the beams, at a most probable relative collision energy of ~63 meV (for CH_4, NH_3, and H_2O) or 64.1 meV (for SF_6). The corresponding de Broglie wavelengths are ~0.64 Å for the first three systems and 0.58 Å for the latter one. Measurements were also made for out-of-plane scattering below the plane of the beams, in order to locate accurately the zero position of the scattering scale (see above). Long-term drifts in beam intensities and detection efficiency were compensated for by periodic measurements of the scattering signal at a reference angle near 5°. The experimentally measured DCS's are shown in Fig. 1 for $He + CH_4$, $He + NH_3$, and $He + H_2O$, and in Fig. 2 for $He + SF_6$.[15]

The data reduction procedure used to obtain the fits shown in Figs. 1 and 2 has been described previously.[4] It consists of a standard weighted nonlinear least-squares optimization[16] of the parameters of mathematical functions chosen to represent the intermolecular potential, as discussed in Sec. III. As in previous work, appropriate velocity and angle averaging is included in the

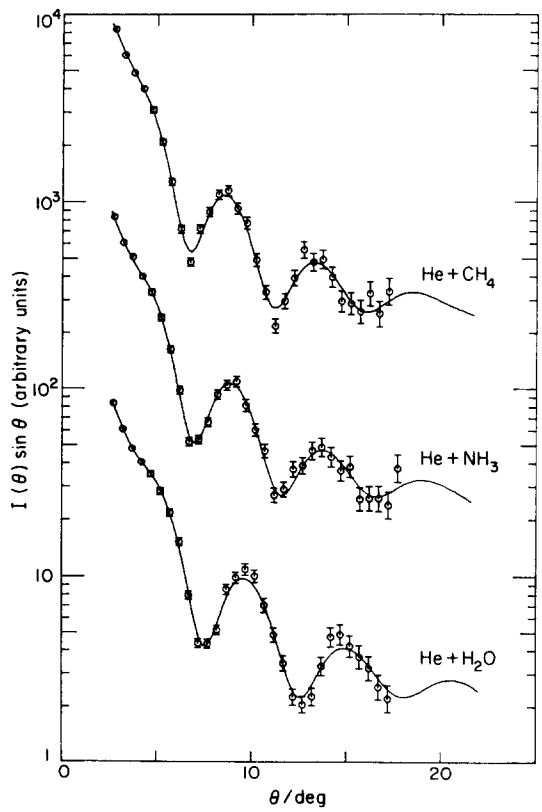

FIG. 1. Laboratory differential cross sections $I(\theta)$[15] for out-of-plane scattering of He by CH_4, NH_3, and H_2O. These curves are successively shifted downwards by one decade for clarity of display. Points with error bars are the experimental measurements of $I(\theta)\sin\theta$ vs the scattering angle θ at a relative collision energy of 63 meV. Solid curves are DCS's calculated from the best-fit central-field SPFD potentials, whose parameters are given in Table II.

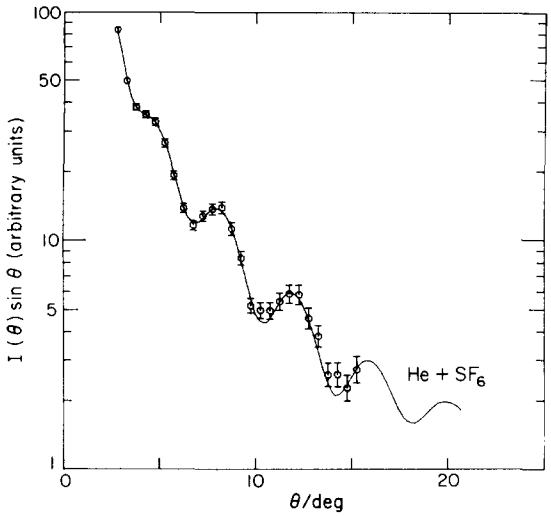

FIG. 2. Laboratory differential cross sections[15] for out-of-plane scattering of He by SF_6 at a relative collision energy of 64 meV. Symbols are as in Fig. 1.

DCS calculations. The overall apparatus relative velocity resolution is ~15% FWHM for $He+CH_4$, NH_3, H_2O, and ~11% FWHM for $He+SF_6$; the overall apparatus angular resolution is 1.9° FWHM.[4]

The least-squares parameter optimization minimizes the functional

$$\chi^2=\sum_{i=1}^{n} g_i(I_i-\alpha\sigma_i)^2 \ . \tag{1}$$

As in our earlier studies, we define a goodness-of-fit statistical index more suitable than χ^2 for describing the quality of the fits to the DCS by

$$\Delta\alpha_{0.95}/\alpha=(1/\alpha)\,t_{0.05}(n-k)\left[\frac{\chi^2}{(n-k)\sum_{i=1}^{n} g_i\sigma_i^2}\right]^{1/2} \ . \tag{2}$$

In these equations, I_i and σ_i are the measured (arbitrarily normalized) and calculated (absolute) cross sections[15] at each of n scattering angles, respectively, with the normalized weights g_i. For n data points and k parameters, $t_{0.05}(n-k)$ is the appropriate Student t-distribution statistic for a 95% confidence level of the scaling factor α.[17] We point out that the $\Delta\alpha_{0.95}/\alpha$ statistical index is independent of the arbitrary normalization used in the experiment. Furthermore, it is statistically adjusted for the number of data points and fitted parameters, which should allow a more straightforward comparison between different potential forms, and between scattering results from different laboratories.

III. DATA ANALYSIS AND INTERMOLECULAR POTENTIALS

The experimental DCS's measured as described in Sec. II and displayed in Figs. 1 and 2 were fitted by a least-squares procedure, using the intermolecular potential forms described below. These are written in the reduced form,

$$f(\rho)=\frac{V(r)}{\epsilon} \ , \qquad \rho=\frac{r}{r_m} \ , \tag{3}$$

where r_m is the radius of the attractive minimum and ϵ is its depth. The zero of the potential, occurring at $r=\sigma$, is related to r_m and the potential shape $f(\rho)$, and is not an independent parameter. The intermolecular distance r is usually regarded as the separation between the He atom and the molecular center of mass. For the anisotropic interactions considered in the present study, alternate choices for the origin of r, such as the molecular center of charge, could also be considered. Among the mathematical shape functions $f(\rho)$ used in the present study is the familiar LJ12-6 potential, in order to allow a comparison with the results of integral scattering measurements for $He+CH_4$,[18] and of other DCS results for $He+NH_3$ and $He+N_2O$.[19] More flexible parametric forms for $f(\rho)$ are however, required to accurately describe the weak van der Waals interactions being studied.[12,20] One such potential function is the Morse–spline–van der Waals (MSV) parametrization,[21] given by

$$\left.\begin{aligned} f(\rho)&=e^{\beta(1-\rho)}[e^{\beta(1-\rho)}-2] \quad \text{for } \rho\leq\rho_1 \\ f(\rho)&=(\rho_2-\rho)[s_1(\rho_2-\rho)^2+s_3]+(\rho-\rho_1)[s_2(\rho-\rho_1)^2+s_4] \\ &\qquad \text{for } \rho_1<\rho<\rho_2 \\ f(\rho)&=-\sum_{i=1}^{3} c_{2i+4}\rho^{-(2i+4)} \quad \text{for } \rho\geq\rho_2 \ . \end{aligned}\right\} \tag{4}$$

The cubic spline coefficients s_i $(i=1-4)$ are fixed by smoothness conditions at the spline points ρ_1 and ρ_2, with the first one being chosen as the inflection point of the Morse function, $\rho_1=1+\beta^{-1}\ln 2$.

It has recently been shown that, for room-temperature DCS measurements of the type being considered in the present study, up to five independent potential parameters may be determined.[20] For these parameters to be statistically independent of each other, and hence physically meaningful, the mathematical form of the potential in which they are used must be appropriately flexible. For the experiments considered herein, the shape of the attractive minimum region, to which the DCS data are highly sensitive, must be adjustable independently of the adjacent regions. In particular, for systems with a collision energy relative to ϵ of ~30 (however, see also Sec. IV), the DCS data are somewhat sensitive to the weakly repulsive wall (up to $V\simeq 8$ meV), requiring a parametric form that decouples this region from the attractive well.[20] Consequently, we also analyze the data using a modification of the MSV potential, having a second Morse function joined smoothly to the first at $r=\sigma$. In the resulting M^2SV potential,[22] the additional Morse parameter β' is used exclusively to describe the shape of the repulsive wall. Another parameterization that successfully decouples the attractive minimum region from adjacent regions of the potential is the third-order Simons–Parr–Finlan Dunham (SPFD) potential,[23] and is given by

$$\left.\begin{aligned} f(\rho)&=b_0\lambda^2\left(1+\sum_{i=1}^{3} b_i\lambda^i\right)-1 \quad \text{for } \lambda=1-1/\rho \text{ and } \rho<\rho_f \\ f(\rho)&=-\sum_{i=1}^{3} c_{2i+4}\rho^{-(2i+4)} \quad \text{for } \rho\geq\rho_f \ . \end{aligned}\right\} \tag{5}$$

The two highest-order SPFD coefficients b_2 and b_3 are

fixed by smoothness conditions[24] at the value of $\rho_f = 1.6$.[4,20]

Although some of the dispersion coefficients have been calculated for the interactions of the three lighter molecular partners with He,[25,26] we felt it best to fit this region of the potential empirically, for reasons discussed below. By fixing $c_8 = c_{10} = 0$ in Eqs. (4) and (5), we obtain "effective" dispersion constants C_6' for each interaction pair. We expect these C_6' ($= \epsilon r_m c_6$) to be somewhat greater than the corresponding correct C_6 constants, because of our neglect of higher-order contributions. This neglect may have a substantial effect on the long-range part of the potential, especially for interactions of He with the highly polar molecules NH_3 and H_2O. These should have large r^{-7} contributions to the dispersion energy, which have been estimated as ~30% of the r^{-6} component (at $\rho = 1.6$), even for the nonpolar $He + CH_4$ interaction.[26] However, the sensitivity of the present DCS data to the intermolecular potential is restricted to reduced distances $\rho \gtrsim 1.7$, since very low-angle scattering data are lacking.[20] Because we use the dispersion expansion only for $\rho \gtrsim 1.6$, the $C_6' r^{-6}$ representation should provide a reasonable approximation to that part of the long-range potential which affects our DCS scattering measurements. For these reasons, the C_6 parameter is permitted to vary in these fits instead of being fixed at its theoretical value. The MSV potential thus has four adjustable parameters (r_m, ϵ, β, and c_6), while the M^2SV and SPFD potentials each have five (r_m, ϵ, β, β', and c_6; r_m, ϵ, b_0, b_1, and c_6, respectively).

A prerequisite for Eq. (3), together with the reduced potential forms of Eqs. (4) and (5), to provide an accurate description of the intermolecular interactions of the systems considered in the present paper, is that anisotropic contributions to the potential must be small over the intermolecular distance range to which the DCS data are sensitive. Although this central-field assumption may not be made *a priori* for the analysis of atom–molecule scattering experiments,[10] we nevertheless base our extraction of intermolecular potentials on it. This procedure is justified in the following discussion (Sec. IV).

IV. DISCUSSION

The van der Waals interactions for the atom–molecule systems considered here are anisotropic. As such, the central-field potentials generically represented by Eq. (3) provide at best an approximate description of these interactions. Consequently, the first problem to be addressed is the validity of the central-field assumption.

Even if this assumption were invalid within the range of intermolecular distances sampled, Eq. (3) could still be expected to provide an "effective" description of processes which occur on a time scale much slower than molecular rotations. Any such process would sample only the spherical average of the anisotropic potentials for sufficiently weak interactions. Such processes do not, however, include the present scattering experiments. Typical rotation frequencies of the molecules in the secondary beams used in the present studies are $\sim 10^{12}$ Hz for the hydrides and $\sim 5\times10^{10}$ Hz for SF_6. Under the present experimental conditions, the collision interaction time (to traverse ~8 Å) is $\sim 5\times10^{-13}$ s, corresponding to only about half a revolution during the collision for the hydride molecules, whereas the SF_6 molecule remains essentially motionless. The inversion frequency of NH_3 is ~50 times slower than its rotation frequency, and therefore does not contribute to averaging of the interaction.

Interpretations of scattering results for anisotropic interactions have been based for some time on semiclassical calculations.[27] However, this theory is inappropriate for the highly quantum systems studied herein. As an example of the differences between semiclassical and quantal scattering, we note that the present DCS's exhibit strong undulations well beyond the classical rainbow angle (at ~4° for these systems); semiclassical oscillations should not appear on the dark (wide-angle) side of the rainbow[8c,28] unless the effect of complex trajectories is included.[29] In the present study, we predicate our analysis on a recent empirical, quantitative validation of the central-field assumption for highly quantum systems that are only weakly anisotropic.[10] In that study (Paper III of this series), it was found that the DCS's for $He + N_2$, O_2, CO, and NO showed little evidence for quenching of the observed rapid quantum oscillations that is expected for anisotropic potentials both semiclassically[27] and quantum mechanically,[30] and that has recently been observed for scattering in highly anisotropic systems (e.g., $He + CO_2$).[11] This lack of quenching is equally evident for other H_2, D_2, and He collisions with weakly anisotropic molecules.[8] Moreover, the results of Paper III showed that the spherical averages of the anisotropic potentials extracted from an infinite-order sudden approximation[30a] analysis of the DCS data presented there were indistinguishable, within experimental error, from the potentials obtained by accurate central-field analyses of those data. This is true despite a van der Waals attractive minimum distance that was found to be up to 20% greater for linear configurations than for perpendicular ones. From this it was concluded that a central-field analysis does indeed yield the spherically symmetric component of the interaction potential. This conclusion is valid for weakly anisotropic systems showing little evidence (according to the quantitative criteria given in Paper III) for quenching of the rapid oscillatory structure characteristic of central-field elastic scattering of highly quantum systems. This had previously been supposed for molecular scattering.[8] Unfortunately, a quantitative validation of this result for the present polyatomic systems would be difficult, because too many parameters would be needed to adequately model the corresponding potentials (e.g., two angular degrees of freedom, strong polar effects, etc.). Consequently, we may apply only the qualitative aspects of the conclusions enumerated above to the present study. We first discuss the results for the hydride partners, and treat the $He + SF_6$ interaction somewhat separately later in this section.

TABLE II. Central-field intermolecular potentials fit to the experimental DCS's.

System[a]	Potential type[b]	r_m/Å	σ/Å	ϵ/meV	Shape parameters[c]	Q^d/Å^2	$\chi^{2\,e,f}$	$\Delta\alpha_{0.95}/\alpha^f$(%)
He + CH_4 (30)	MSV	3.86	3.41	2.42	$\beta = 6.01$; $c_6 = 2.20$	95	340(4)	2.73
	M^2SV	3.90	3.40	2.06	$\beta = 5.43$; $\beta' = 10.2$; $c_6 = 1.92$	88	270(5)	2.46
	SPFD	3.80	3.40	2.00	$b_0 = 36.2$; $b_1 = -5.96$; $c_6 = 2.10$	86	250(5)	2.39
He + NH_3 (31)	MSV	3.76	3.29	2.48	$\beta = 5.54$; $c_6 = 2.23$	91	200(4)	2.13
	M^2SV	3.82	3.28	2.03	$\beta = 4.94$; $\beta' = 9.57$; $c_6 = 1.86$	83	140(5)	1.83
	SPFD	3.73	3.28	2.08	$b_0 = 27.5$; $b_1 = -4.98$; $c_6 = 2.19$	84	150(5)	1.89
He + H_2O (30)	MSV	3.46	3.03	2.71	$\beta = 5.54$; $c_6 = 2.40$	80	210(4)	2.53
	M^2SV	3.50	3.01	2.31	$\beta = 5.02$; $\beta' = 10.6$; $c_6 = 2.01$	73	160(5)	2.24
	SPFD	3.38	3.01	2.27	$b_0 = 31.4$; $b_1 = -6.15$; $c_6 = 2.30$	71	150(5)	2.16
He + SF_6 (26)	MSV	4.24	3.75	4.68	$\beta = 6.10$; $c_6 = 1.25$	220	100(4)	1.46
	M^2SV	4.23	3.76	4.68	$\beta = 6.15$; $\beta' = 5.07$; $c_6 = 1.29$	220	90(5)	1.43
	SPFD	4.23	3.77	4.79	$b_0 = 39.8$; $b_1 = -4.62$; $c_6 = 1.31$	220	90(5)	1.46

[a]Experimental conditions given in Table I; the number of experimental data points is given in parentheses.
[b]Defined in Eqs. (3)–(5).
[c]Symbols have the same meanings as in Eqs. (3)–(5) of the text. The MSV and M^2SV potentials also have $\rho_2 = 1.60$; the SPFD potential similarly has $\rho_f = 1.60$. The dispersion constant C_6' is obtained from the fitted reduced dispersion coefficient c_6, where $C_6' = \epsilon r_m^6 c_6$. The prime denotes an effective dispersion coefficient, obtained by neglecting contributions from higher-order multipole terms (see text).
[d]Integral cross sections at a relative collision energy of 63 meV (for He + CH_4, NH_3, H_2O) or 64 meV (for He + SF_6) calculated from the partial wave expansion and the potentials given.
[e]Scattering intensity normalized to 500 at $\theta = 4.8°$ (which differs from the arbitrary normalizations used in Figs. 1 and 2). The number of parameters varied is given in parentheses.
[f]See Eqs. (1) and (2).

A. He + CH_4, NH_3, and H_2O interactions

Potential parameters obtained from central-field analyses of the He + CH_4, NH_3, and H_2O DCS's are presented in Table II. As in previous work, it may immediately be seen that the five-parameter M^2SV and SPFD potentials are better able to fit the DCS data for these three systems than is the MSV model, even when the use of one additional parameter in the former potentials is statistically accounted for[4] (see $\Delta\alpha_{0.95}/\alpha$ column of Table II). Again as in previous work, the well position parameters are largely model independent (± 0.06 Å for r_m and ± 0.01 Å for σ); however, ϵ values obtained by using the MSV potential model are consistently ~ 20% greater than for the M^2SV of SPFD potentials. Despite the different mathematical parameterizations of the latter two potentials, they both have the appropriate flexibility (see also Séc. III) to allow ϵ to be determined with an accuracy of about ± 10%[20]; indeed the M^2SV and SPFD values of ϵ for the He + CH_4, NH_3, and H_2O systems are different by only ~ 2%. We also display in Table II the integral cross sections Q at a relative collision energy of 64 meV, calculated for these three systems using the partial wave expansion. Because of the consistently greater well depths of the MSV potentials, their Q are about 10% larger than those of the corresponding M^2SV or SPFD potentials.

The quality of even the five-parameter fits to the He + CH_4, NH_3, and H_2O experimental DCS's unfortunately is not quite as good as could be hoped for ("good" fits furnish $\Delta\alpha_{0.95}/\alpha \lesssim 2.2\%$[20]). By comparing the calculated DCS's to the experimental ones, as in Fig. 1, we see however, that there is no evidence for quenching of the oscillations in the experimental DCS relative to those calculated using central-field potentials. If anything, the experimental DCS's have slightly greater oscillatory amplitudes than do the calculated ones (cf. the first and second minima of He + CH_4, and the first and second maxima of He + H_2O). In any case, all three systems yield ϵ and r_m values that are very close to those of other atomic[7,12,31] and molecular[10,19] interactions with He. Since there is thus no evidence for significant anisotropic contributions to the measured DCS's, we conclude[10] that the central-field analysis yields the spherically symmetric component of the intermolecular potential, for the range of reduced distances probed in these experiments ($0.8 \lesssim \rho \lesssim 1.7$).

The He + CH_4 interaction potential has previously been studied by (arbitrarily normalized) integral scattering cross section measurements Q, as a function of the collision velocity v.[18] An LJ12-6 analysis of these data yielded a value of ϵr_m as a measure for the "area" of the attractive well. As an indication of the consistency between those $Q(v)$ measurements and the present DCS results, we display in Table III values of ϵr_m for He + CH_4 as determined from both these experiments (within the LJ12-6 parameterization). The agreement is seen to be quite satisfactory; we also present ϵr_m values for our more accurate five-parameter potentials. In addition, we compare in Table III our fitted "effective" C_6' dispersion coefficients (Sec. III) with those obtained theoretically.[25,26] The experimentally determined coefficients for He + CH_4, NH_3, and H_2O are seen to be ~ 70% greater than for the corresponding calculated ones. Although this discrepancy is rather large, it is not unexpected, and is caused primarily by our neglect of higher-order contributions to the dispersion interaction (Sec. III).

Finally, we compare in Table III r_m and ϵ parameters obtained from LJ12-6 analyses of the present DCS re-

TABLE III. Potential parameters obtained from DCS results, integral cross section measurements, and calculated dispersion coefficients.

Potential quantity	System				Error	Method of determination	Ref.
	He + CH_4	He + NH_3	He + H_2O	He + SF_6			
ϵr_m/(meV Å)	9.0	•••	•••	•••	0.6	$Q(v)$[a]	18
	8.9	9.0	9.3	23	•••	DCS[a]	this work
	7.8	7.8	7.9	20	0.2	DCS[b]	this work
C_6/(eV Å^6)	7.9	6.6	4.8	•••	•••	calculated[c]	25
	8.9	•••	•••	•••	•••	calculated[c]	26
	6.6	5.6	4.5	22	•••	calculated[d]	32
C_6'/(eV Å^6)	13	12	8	35	2	DCS[e]	this work
σ[f]/Å	•••	3.09	2.98	•••	0.06	DCS[a]	19
	3.40	3.28	3.02	3.75	0.03	DCS[a]	this work
ϵ/meV	•••	2.2	2.5	•••	0.3	DCS[a]	19
	2.3	2.5	2.7	5.6	•••	DCS[a]	this work

[a]Using the LJ12-6 potential.
[b]Using the M^2SV and SPFD potentials; the error reflects the discrepancies among the ϵr_m products for these potential forms.
[c]Spherically symmetric contributions to C_6.
[d]From the approximate formulae of Ref. 32 in terms of static polarizabilities, ionization energies, and dipole moments.
[e]Using the M^2SV and SPFD potentials, and neglecting contributions of higher order than C_6 to the dispersion interaction. The error reflects the ± 20% or poorer accuracy with which the "attractive tail" portion of the potential ($r \gtrsim 5$ Å) is determined[20] for the He + CH_4, NH_3, H_2O systems. See Sec. IV. B for a discussion of the corresponding error in C_6' for He + SF_6.
[f]For the LJ12-6 potential, $\sigma = 2^{-1/6} r_m$.

sults, and those of another laboratory.[19] All these experiments were performed at about the same relative collision energy (60 ± 4 meV), and for about the same range of scattering angles (2° or 3° to ~ 18°). Data reduction using the same potential form should allow a fairly direct comparison between these results, although we caution that the LJ12-6 parameterization is too rigid to yield accurate intermolecular potentials for the interactions being considered. We see that the He + H_2O results agree well, but that the σ (or r_m) parameters for He + NH_3 differ substantially. A similar discrepancy also exists for H_2 + NH_3 scattering, where again the Waterloo results[19] yielded a significantly smaller σ (or r_m) parameter than obtained in this laboratory.[8c] We have conducted very extensive self-consistency checks of our measurements[4] comparable to those of the Waterloo group.[19] We have also established the compatibility of our in-plane and out-of-plane measurements (the latter geometry is kinematically identical to the out-of-plane scattering geometry used by the Waterloo group). Nevertheless, the experimental (H_2, He) + NH_3 scattering data of the two laboratories still appear to be somewhat inconsistent. That the discrepancy appears only for scattering of NH_3, but not for the He + H_2O or He + Ar systems,[4,12] indicates that the cause may lie in the secondary beam composition. We have already eliminated the possibility of NH_3 beam impurities, particularly with respect to dimerization, by highly sensitive mass spectrometric checks (Sec. II). To compare the quality of the fit to the data, we may renormalize (see footnote e of Table II) the scattering intensity of the present DCS results (fit to the LJ12-6 potential) to those obtained previously.[19] We find a goodness-of-fit statistic of $\chi^2 = 17.9$ [Eq. (1)], even with four data points more than the Waterloo experiment, which yielded a corresponding value of $\chi^2 = 38.3$. The difficulty in the fit to the latter experiment is evident for scattering angles beyond ~ 10°, where the experimental DCS is systematically higher than the calculated one.[19] It is possible that the above differences are caused more by the rigidity of the LJ12-6 potential form than by inconsistencies between the data; more flexible potential forms are needed to attain appropriate descriptions of DCS scattering results[20] from the two laboratories (such as the M^2SV and SPFD potentials used in this study).

In the above comparison between the present results and potentials obtained previously, we have ignored bulk property data. This is because the latter are usually sensitive only to interactions more repulsive than those sensitively probed by the present thermal scattering experiments.[4] Moreover, the effect of potential anisotropies on bulk properties has not yet been investigated to a sufficient extent.[30a]

We now discuss systematic trends among the accurate five-parameter potentials extracted from the present He + CH_4, NH_3, and H_2O DCS data. The SPFD potentials for these systems are displayed in Fig. 3; the M^2SV potentials are indistinguishable from the former within experimental error and are not plotted. Two features are clearly apparent from a comparison of these curves. Most evident is that the repulsive walls for the three systems are displaced to smaller intermolecular separations in the order $CH_4 > NH_3 > H_2O$. This trend is correlated with the H ··· H nonbonded distance, and thus to the molecular size. We also notice that continuing in

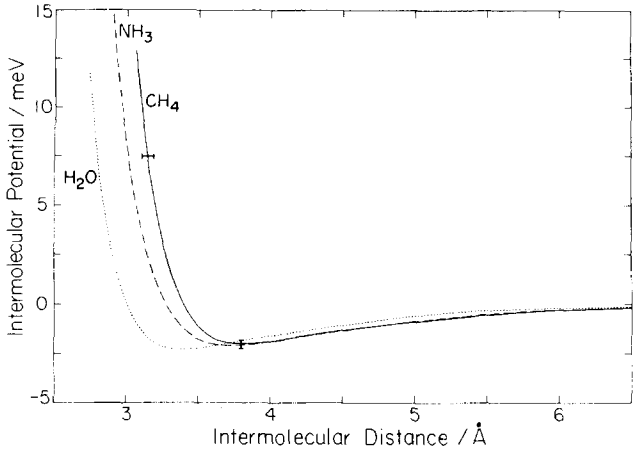

FIG. 3. Central-field intermolecular potentials of the SPFD shape, corresponding to the He + CH_4, NH_3, and H_2O DCS fits of Fig. 1, as a function of the intermolecular distance (see Sec. III for a discussion of the definition of this distance). Solid curve: He + CH_4; dashed curve: He + NH_3; dotted curve: He + H_2O. The error bars on the He + CH_4 potential represent the accuracy with which it has been determined, ± 10% of the potential energy at the attractive minimum, ± 0.04 Å in the position of the repulsive wall at ~ 7.5 meV. The potentials are plotted over the approximate range of distances to which the experiments are sensitive.[20]

this isoelectronic series, the He + Ne interaction has σ = 2.73 Å,[31] 0.28 Å less than for the He + H_2O potential (Table II); accurate He + HF data are not yet available.[33,34] Thus, it appears that although H atoms are ineffective in promoting anisotropies in the interaction of He with CH_4, NH_3, and H_2O, they do increase the apparent size of these molecules. It may be that the lone-pair electrons of NH_3 and H_2O contribute to the apparent isotropicity of the interactions of these molecules with He, despite their rather asymmetric nuclear arrangements.

The second trend displayed by the potentials of Fig. 3 is evident in their long-range regions. We see that the strength of the attractive potential for $r \lesssim 4$ Å falls in the sequence $CH_4 \simeq NH_3 > H_2O$. This is also reflected by the calculated C_6 constants (see Table III).[25] The calculated long-range potential is dominated by induced dipole-induced dipole, rather than by dipole-induced dipole, dispersion forces. The former accounts for 90% of the He + NH_3 C_6 coefficient and 80% of the He + H_2O one.[32] The permanent dipole moments of NH_3 and H_2O thus do not substantially affect their long-range interactions with He, as is also reflected by the experimental potentials of Fig. 3.

B. The He + SF_6 interaction

We discuss this system separately from the He + CH_4, NH_3, and H_2O ones primarily because of the much larger well depth for He + SF_6, as is evident from the potential parameters presented in Table II. We note that this well depth is more than twice that for most other molecular interactions with He,[10,19] having the important consequence of reducing the collision energy from ~ 30 to ~ 13 ϵ. For a system with a well depth of $\epsilon \simeq 2$ meV, the latter value corresponds to a collision energy of ~ 25 meV. Consequently, we expect the He + SF_6 DCS to be more sensitive to the long-range region of the intermolecular potential than are those of the other systems considered here. Computer simulation calculations[20] (with which the He + CH_4, NH_3, and H_2O systems were compared) lead us to expect our He + SF_6 potential to have somewhat better than 20% accuracy for reduced distances ρ between about 1.4 and 1.6. Those simulations also indicate that our determination of the He + SF_6 well depth should still be accurate to ~ 10%. Furthermore, the He + SF_6 DCS should be rather insensitive to the repulsive wall, and so the M^2SV and SPFD potential forms should effectively have about the same flexibility as does the MSV potential. This effect has been shown to occur for low collision energy (~ 9 ϵ) interactions in highly quantum systems.[20] Indeed, the MSV potential parameters displayed in Table II show no bias toward a larger well depth than is obtained from the M^2SV and SPFD analyses, and no improvement in fitting quality is seen. The corresponding integral cross sections also show no bias (see Sec. IV A). It may be more appropriate to introduce greater flexibility into the long-range region by using a dispersion term of higher order than C_6. We also note that the He + SF_6 potential predictably has a rather large range parameter r_m. The He + SF_6 potential extracted from the present DCS results is displayed in Fig. 4.

Among the systems investigated here, the He + SF_6 DCS gives the best potential fit (Table II): there is again no evidence in that fit for quenching of the rapid quantum oscillatory structure (Fig. 2). We conclude that the present He + SF_6 data are insensitive to anisotropic components of the potential, which probably only become evident for repulsive interactions. The large ϵ observed for this system may be due to interactions with the F atoms. It would be interesting to conduct a scattering study of He + CF_4 to elucidate the nature of such

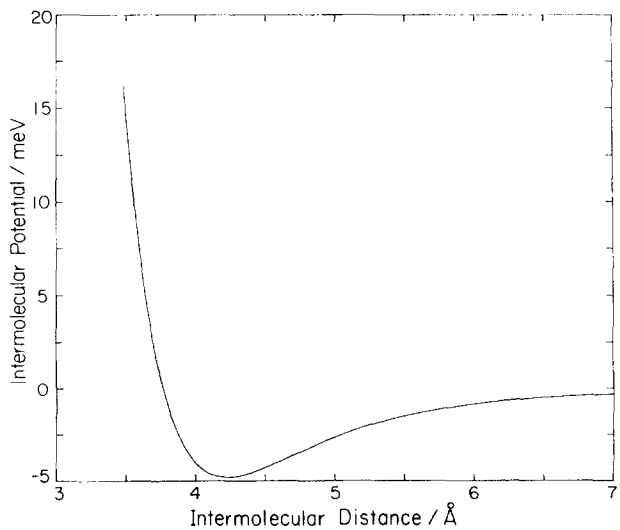

FIG. 4. Central-field intermolecular potential of the SPFD shape, corresponding to the He + SF_6 fit of Fig. 2, as a function of the intermolecular distance (see Sec. III for a discussion of the definition of this distance). The accuracy of this potential is discussed in Sec. IV. B. The range of validity of this potential is approximately 3.7 Å ($V \gtrsim 5$ meV) to 7 Å.

TABLE IV. Potential parameters from simple combination rules compared with experiment.

System[a]	σ_{jj}/Å	σ_{ij}[b]/Å	σ_{ij}[c]/Å	ϵ_{jj}/meV	ϵ_{ij}[d]/meV	ϵ_{ij}[e]/meV	ϵ_{ij}[c]/meV
He + CH_4[f]	3.43	3.06	3.40	20	4.3	3.9	2.0
He + NH_3[g]	3.15	2.92	3.28	31	5.3	2.6	2.1
He + NH_3[h]	3.42	3.06	3.28	14	3.6	3.3	2.1
He + H_2O[g]	2.71	2.70	3.01	44	6.3	3.3	2.3
He + H_2O[h]	3.06	2.88	3.01	17	3.9	3.8	2.3
He + SF_6[f]	4.53	3.61	3.77	36	5.7	3.6	4.7

[a]For He_2, $\sigma_{ii} = 2.69$ Å, $\epsilon_{ii} = 0.91$ meV, from Ref. 1(d).
[b]$\sigma_{ij} = \frac{1}{2}(\sigma_{ii} + \sigma_{jj})$.
[c]Present experiments, average of M^2SV and SPFD potential fits.
[d]$\epsilon_{ij} = (\epsilon_{ii}\epsilon_{jj})^{1/2}$.
[e]$\epsilon_{ij} = 2\alpha_i\alpha_j/\sigma_{ij}^6(\gamma_i + \gamma_j)$, where $\gamma_k = \alpha_k^2/\epsilon_{kk}\sigma_{kk}^6$ $(k = i, j)$; α_k is the spherically averaged polarizability and σ_{ij} is obtained from the combination rule of footnote b.
[f]Homomolecular parameters from Ref. 38.
[g]Homomolecular parameters from Ref. 39.
[h]Homomolecular parameters from Ref. 40.

interactions. It is also possible that the *d* orbital of the S atom plays a role in governing the nature of the van der Waals attractive interactions. Note however, that the spherically symmetric $H_2(D_2) + SF_6$ van der Waals interaction has about the same ϵ as do the $H_2(D_2) + NH_3$ and $H_2 + CH_4$ interactions.[8c] The $He + SF_6$ potential thus provides a clear counter example of previous empirical observations that it is primarily the least polarizable partner that is responsible for the magnitude of the van der Waals well depth.[31]

The effect of the large r_m and ϵ parameters on $He + SF_6$ scattering is apparent from the fact that the DCS of Fig. 2 is significantly different from those of Fig. 1. The residual rainbow at ~4° is more evident than in the $He + CH_4$, NH_3, and H_2O DCS's while the amplitude of the rapid quantum oscillations is comparably diminished. We also see a closer spacing of these oscillations, expected from their reciprocal relationship to the reduced collision wavenumber, which in turn is directly proportional to r_m.[28]

C. Combination rule predictions

Historically, the incentive for the extensive development of combination rules—only some of which are based soundly upon theoretical or experimental considerations[32–35]—may in part be attributed to difficulties in the bulk sample measurements of unlike-pair properties. The validity of such rules is predicated upon the existence of a single reduced form or "universal function" for the interaction pairs being considered. The existence of such a universal function is related to the "law of corresponding states" for the equation of state of real gases.[32] Together with values for the distance and energy scaling parameters (σ or r_m and ϵ, respectively) appropriate for each of these interactions, the corresponding potential energy functions would then be predictable. However, the concept of such universal functions has been shown to be inappropriate for potentials determined accurately by other means[3d,20]; the validity of various combination rules for predicting potential parameters for unlike-pair interactions from the constituent like-pair ones has been discussed extensively for atom–atom potentials.[3d,4,7,31,36]

Combination rules for describing interactions in molecular systems ignore anisotropic contributions to the interaction potential and consider only their spherically symmetric components. As discussed earlier, this approximation is valid for the present atom–molecule systems for the range of intermolecular distances sampled by our experiments, but the validity of the central-field assumption for the constituent like-pair molecule–molecule interactions is uncertain. Moreover, experimental determinations of homomolecular interaction potentials have yielded widely different values for the potential parameters.[37]

As a quantitative indication of the difficulties encountered in using combination rules to accurately predict potential parameters for unlike-pair interactions, we compare in Table IV the present experimental determinations of σ and ϵ to the results of several commonly used simple combination rules. The like-pair potential parameters are based on a variety of potential energy functional forms. It may easily be seen that the predictions for σ are consistently too low, even when [for $(NH_3)_2$ and $(H_2O)_2$] the wide range of like-pair experimental results are considered. Similarly, the predictions for ϵ are consistently too high (except for $He + SF_6$). The failure of the combination rules is in all cases beyond the experimental error of ±1% in our determination of σ, and ±10% in ϵ.[20] The use of combination rules should therefore be restricted to those interactions for which accurate potentials are unavailable, and must not be considered reliable.[3a]

V. SUMMARY AND CONCLUSIONS

Van der Waals potentials for the interactions of He atoms with molecules of CH_4, NH_3, H_2O, and SF_6 have been extracted from differential cross sections (DCS), as measured by the crossed-beams technique. For sys-

tems showing only weak anisotropies, a suitable central-field analysis yields the spherically symmetric component of the interaction potential.[10] The present DCS's show no evidence of quenching, which has been predicted,[30] and observed,[11] for molecular scattering in highly anisotropic quantum systems. Hence we conclude that the central-field potentials extracted from the data are good representations for the spherically symmetric components of the $He+CH_4$, NH_3, H_2O, and SF_6 interactions, and that anisotropic components are small for the attractive, and even weakly repulsive, regions of their potentials.

We find a simple correlation between molecular size and the van der Waals radii of the $He+CH_4$, NH_3, and H_2O interactions, which fall in the sequence $CH_4 > NH_3 > H_2O$. This sequence may be extended to the isoelectronic He + Ne interaction,[31] whose size is even less than that of $He+H_2O$. We find no substantial effect of the large dipole moments of NH_3 and H_2O upon the long-range attractive potential. The $He+SF_6$ potential is found to violate the usual supposition[31] that only the least polarizable of the interacting atoms (or molecules) are correlated with the van der Waals well depth.

Simple combination rules for predicting values of the well depth ϵ and interaction distance σ $[V(\sigma)=0]$ of unlike pairs from the corresponding like-pair potential parameters are tested and found inadequate.

ACKNOWLEDGMENT

We wish to thank Ambassador College for generous use of its computing facilities.

[1]For examples, see (a) I. Amdur and J. E. Jordan, Adv. Chem. Phys. **10**, 29 (1966); (b) J. M. Parson, P. E. Siska, and Y. T. Lee, J. Chem. Phys. **56**, 1511 (1972); (c) D. E. Freeman, K. Yoshino, and Y. Tanaka, *ibid.* **61**, 4880 (1974); (d) A. L. J. Burgmans, J. M. Farrar, and Y. T. Lee, *ibid.* **64**, 1345 (1976), and references quoted in these papers.

[2](a) J. O. Hirschfelder and W. J. Meath, Adv. Chem. Phys. **12**, 3 (1967); (b) Y. S. Kim and R. G. Gordon, J. Chem. Phys. **61**, 1 (1974); (c) J. S. Cohen and R. T Pack, *ibid.* **61**, 2372 (1974); (d) P. D. Dacre, Chem. Phys. Lett. **50**, 147 (1977).

[3]For recent reviews, see (a) U. Buck, Adv. Chem. Phys. **30**, 313 (1975); (b) J. P. Toennies, in *Physical Chemistry: an Advanced Treatise*, Vol. 6A, edited by H. Eyring, D. Henderson, and W. Jost (Academic, New York, 1974), p. 227; (c) G. C. Maitland and E. B. Smith, Chem. Soc. Rev. 2, 181 (1973); (d) Ch. Schlier, Ann. Rev. Phys. Chem. **20**, 191 (1969).

[4]M. Keil, J. T. Slankas, and A. Kuppermann, "Scattering of thermal helium beams by crossed atomic and molecular beams. II. The He–Ar van der Waals potential," J. Chem. Phys. (in press).

[5]D. E. Freeman, K. Yoshino, and Y. Tanaka, J. Chem. Phys. **67**, 3462 (1977).

[6](a) J. H. Dymond and B. J. Alder, J. Chem. Phys. **51**, 309 (1969); (b) R. J. LeRoy, M. L. Klein, and I. J. McGee, Mol. Phys. **28**, 587 (1974); (c) R. A. Aziz and H. H. Chen, J. Chem. Phys. **67**, 5719 (1977).

[7]K. M. Smith, A. M. Rulis, G. Scoles, R. A. Aziz, and V. Nain, J. Chem. Phys. **67**, 152 (1977).

[8]For examples involving molecular scattering of light systems, see (a) D. H. Winicur, A. L. Moursund, W. R. Devereaux, L. R. Martin, and A. Kuppermann, J. Chem. Phys. **52**, 3299 (1970); (b) J. M. Farrar and Y. T. Lee, J. Chem. Phys. **57**, 5492 (1972); (c) A. Kuppermann, R. J. Gordon, and M. J. Coggiola, Faraday Discuss. Chem. Soc. **55**, 145 (1973); (d) R. W. Bickes, G. Scoles, and K. M. Smith, Can. J. Phys. **53**, 435 (1975); (e) A. M. Rulis and G. Scoles, Chem. Phys. **25**, 183 (1977).

[9](a) R. J. LeRoy, J. S. Carley, and J. E. Grabenstetter. Faraday Discuss. Chem. Soc. **62**, 169 (1977); (b) R. E. Smalley, L. Wharton, and D. H. Levy, J. Chem. Phys. **68**, 671 (1978); (c) W. Klemperer, Faraday Discuss. Chem. Soc. **62**, 179 (1977); (d) J. Reuss, Adv. Chem. Phys. **30**, 389 (1975).

[10]M. Keil, J. T. Slankas, and A. Kuppermann, "Scattering of thermal He beams by crossed atomic and molecular beams. III. Anisotropic intermolecular potentials for $He+N_2$, O_2, CO, NO," J. Chem. Phys. (in press), hereafter referred to as Paper III.

[11]M. Keil, G. A. Parker, and A. Kuppermann, "An empirical anisotropic potential for $He+CO_2$," Chem. Phys. Lett. (in press).

[12]M. Keil, A. Kuppermann, and J. T. Slankas, "An accurate determination of the He–Ar van der Waals potential," Chem. Phys. Lett. (to be published).

[13]J. B. Anderson and J. B. Fenn, Phys. Fluids **8**, 780 (1965).

[14]W. L. Fite, *International Conference on Mass Spectroscopy*, Kyoto, Japan (1969), edited by K. Ogata and T. Hayakawa (University Park, Baltimore, 1971), p. 1001; R. E. Leckenby and E. J. Robbins, Proc. R. Soc. London Ser. A **291**, 389 (1966).

[15]It is convenient to refer to $I(\theta)$ as a laboratory differential cross section in arbitrary units. However, $I(\theta)$ is really a signal intensity. To transform it into such a laboratory DCS requires multiplication by the laboratory velocity of the scattered beam (which is a function of θ), since the mass spectrometer used in our measurements is a number density detector. See Ref. 4 for details.

[16]D. W. Marquardt, J. Soc. Ind. Appl. Math. **11**, 431 (1963).

[17]N. R. Draper and H. Smith, *Applied Regression Analysis* (Wiley, New York, 1966), Chaps. 2 and 9.

[18]H. P. Butz, R. Feltgen, H. Pauly, and H. Vehmeyer, Z. Phys. **247**, 70 (1971).

[19]R. W. Bickes, G. Duquette, C. J. N. van den Meijdenberg, A. M. Rulis, G. Scoles, and K. M. Smith, J. Phys. B **8**, 3034 (1975).

[20]M. Keil and A. Kuppermann, "Scattering of thermal He beam beams by crossed atomic and molecular beams. I. Sensitivity of the elastic differential cross section to the interatomic potential," J. Chem. Phys. (in press).

[21]J. M. Parson and Y. T. Lee, Entropie **42**, 146 (1971).

[22]Our M^2SV potential is somewhat similar to the MMSV part of the ESMMSV potential form proposed in Ref. 1(d). However, we join the two Morse functions at σ, rather than at r_m.

[23]G. Simons, R. G. Parr, and J. M. Finlan, J. Chem. Phys. **59**, 3229 (1973).

[24]R. W. Bickes and R. B. Bernstein, Chem. Phys. Lett. **26**, 457 (1974).

[25]D. J. Margoliash and W. J. Meath, J. Chem. Phys. **68**, 1926 (1978).

[26]H. N. W. Lekkerkerker, P. Coulon, and R. Luyckx, J. Chem. Soc. Faraday II **73**, 1328 (1977).

[27](a) R. E. Olson and R. B. Bernstein, J. Chem. Phys. **49**, 162 (1968); (b) R. J. Cross, *ibid.* **52**, 5703 (1970).

[28]R. B. Bernstein, Adv. Chem. Phys. **10**, 75 (1966).

[29]R. J. Gordon, J. Chem. Phys. **63**, 3109 (1975).

[30](a) G. A. Parker and R. T Pack, J. Chem. Phys. **68**, 1585 (1978); (b) R. T Pack, Chem. Phys. Lett. **55**, 197 (1978).

[31]C. H. Chen, P. E. Siska, and Y. T. Lee, J. Chem. Phys. **59**, 601 (1973).

[32]J. O. Hirschfelder, C. F. Curtiss, and R. B. Bird, *Molec-*

ular Theory of Gases and Liquids (Wiley, New York, 1954), Chaps. 4 and 13.
[33]H. Lischka, Chem. Phys. Lett. **20**, 448 (1973); Chem. Phys. **2**, 191 (1973).
[34]J. Detrich and R. W. Conn, J. Chem. Phys. **64**, 3091 (1976).
[35]For recently proposed combination rules, see, for example, C. L. Kong, and M. R. Chakrabarty, J. Phys. Chem. **77**, 2668 (1973); F. T. Smith, Phys. Rev. A **5**, 1708 (1972); H. L. Kramer and D. R. Herschbach, J. Chem. Phys. **53**, 2792 (1970); P. T. Sikora, J. Phys. B **3**, 1475 (1970).
[36]C. Y. Ng, Y. T. Lee, and J. A. Barker, J. Chem. Phys. **61**, 1996 (1974).
[37]For a recent compilation of $(NH_3)_2$ potential parameters, see R. Brooks and A. E. Grosser, Mol. Phys. **28**, 593 (1974); for $(H_2O)_2$ see R. Brooks, F. Kalos, and A. E. Grosser, Mol. Phys. **27**, 1071 (1974). For a very recent intermolecular potential function for $(NH_3)_2$, see G. Duquette, T. H. Ellis, G. Scoles, R. O. Watts, and M. L. Klein, J. Chem. Phys. **68**, 2544 (1978); for $(H_2O)_2$ see R. O. Watts, Chem. Phys. **26**, 367 (1977).
[38]I. K. Snook and T. H. Spurling, J. Chem. Soc. Faraday II **68**, 1359 (1972).
[39]L. Monchick and E. A. Mason, J. Chem. Phys. **35**, 1676 (1961).
[40]J. H. Bae and T. M. Reed, Ind. Eng. Chem. Fundam. **6**, 67 (1967).